Letter

Thermodynamic phases in first detected return times of quantum many-body systems

Benjamin Walter [1], Gabriele Perfetto [2,*] and Andrea Gambassi [3]

[1] *Department of Mathematics, Imperial College London, London SW7 2AZ, United Kingdom*

[2] *Institut für Theoretische Physik, Universität Tübingen, Auf der Morgenstelle 14, 72076 Tübingen, Germany*

[3] *SISSA–International School for Advanced Studies and INFN, via Bonomea 265, 34136 Trieste, Italy*

(Received 14 March 2024; revised 14 January 2025; accepted 11 March 2025; published 28 April 2025)

We study the probability distribution of the first return time to the initial state of a quantum many-body system subject to global projective measurements at stroboscopic times. We show that this distribution can be mapped to a continuation of the canonical partition function of a classical spin chain with noninteracting domains at equilibrium, which is entirely characterized by the Loschmidt amplitude of the quantum many-body system. This allows us to conclude that this probability may decay either algebraically or exponentially at long times, depending on whether the spin chain displays a ferromagnetic or a paramagnetic phase. We illustrate this idea on the example of the return time of N adjacent fermions in a tight-binding model, revealing a rich phase behavior, which can be tuned by scaling the probing time as a function of N. The analysis presented here provides an overarching understanding of many-body quantum first detection problems in terms of equilibrium thermodynamic phases. Our theoretical predictions are in excellent agreement with exact numerical computations.

DOI: 10.1103/PhysRevA.111.L040202

Introduction. Understanding the propagation of quantum information in monitored many-body quantum systems is of central importance for quantum simulators [1–5] and computation [6–10]. Thus motivated, the impact of monitoring *local* degrees of freedom in many-body quantum dynamics has recently attracted significant interest, leading to the discovery of measurement-induced phase transitions [11–14]. For quantum computing applications [15–20], however, *global* site-resolved monitoring of the many-body wave function is also fundamental. In spite of this crucial role, the interplay between unitary dynamics and global projective measurements has been rarely investigated so far.

In order to advance in this direction, we tackle this problem by studying the *first detected return time* (FDRT) of quantum many-body systems under global projective measurements at stroboscopic times $\tau, 2\tau, \ldots, k\tau$, see Fig. 1. This "stroboscopic" protocol, studied for single particles in Refs. [21–41], has been implemented on a quantum computer [40–42], demonstrating a potential speedup of quantum search algorithms. For quantum many-body systems, however, analytical results have been obtained for mean values only [43]. For the first detection distribution, results are limited to small system sizes [44,45] due to the exponential complexity of many-body numerical simulations. No analytical understanding of many-body FDRT is currently within reach of established techniques.

In this Letter, we investigate the *full* FDRT distribution F_k for arbitrary many-body systems, deriving exact analytical predictions for it. We do so by devising an exact mapping of the quantum many-body FDRT probability onto the classical partition function of a one-dimensional spin model with noninteracting domains. Similar classical partition functions appear in studies of the DNA melting transitions [46–49], in the truncated inverse distance squared Ising model [50–53], or in nonequilibrium currents [54]. In the mapping we devise, the canonical weight of classical spins is obtained from the many-body Loschmidt amplitude. From the latter, we find that the spins within a magnetic domain feature long-range interactions and thus phase transitions already in one dimension. Specifically, the mapping proposed here allows us

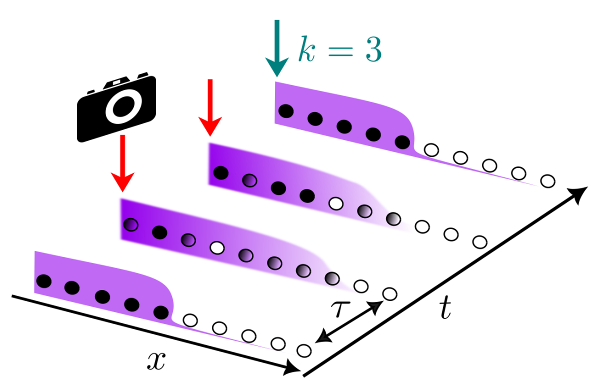

FIG. 1. Illustration of the many-body first detected return protocol: A wave function is prepared in an initial state $|\Psi(0)\rangle$ with N adjacent particles and it evolves unitarily; at stroboscopic times $\tau, 2\tau, \ldots, k\tau$, a projective measurement detects whether or not the state has returned to $|\Psi(0)\rangle$. The first such successful measurement defines the FDRT, here 3τ.

---

[*] Contact author: gabriele.perfetto@uni-tuebingen.de

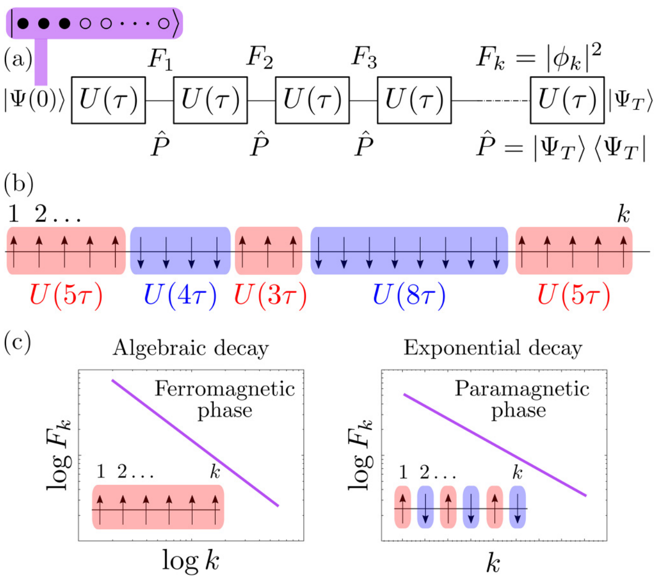

FIG. 2. Mapping between quantum many-body first detection time and statistical mechanics. (a) A wave function evolves with unitary dynamics $U(\tau)$ interspersed by projective measurements $\hat{P}$ occurring at stroboscopic times multiples of τ. The target state $|\Psi_T\rangle = |\Psi(0)\rangle$ is first detected at the kth measurement with first detected return amplitude ϕ_k and probability $F_k = |\phi_k|^2$. The protocol terminates at the first successful detection in $|\Psi_T\rangle$. (b) ϕ_k can be decomposed in terms of time intervals of measurement-free dynamics $U(n\tau)$ (in the figure $n = 5$, 4, 3, 8, and 5, from left to right). Each interval can be mapped into a domain of aligned classical spins, with spins interacting via long-range interactions. Accordingly, ϕ_k is mapped onto a problem of statistical mechanics of domains at equilibrium in a volume k. (*c*) When F_k is determined by long measurement-free intervals $\sim U(k\tau)$, one has a ferromagnetic phase and F_k decays algebraically upon increasing k. Conversely, when short intervals $\sim U(\tau)$ dominate, F_k decays exponentially. This corresponds to the paramagnetic phase.

to classify and understand the different asymptotic decays of F_k as a function of k in terms of the equilibrium phases of the associated classical model. Namely, ferromagnetic ordering is mapped onto algebraic decay of F_k, while paramagnetic behavior corresponds to a faster exponential decay of F_k. We illustrate this approach by considering the case of a domain of N adjacent fermions in a tight-binding model. Different thermodynamic phases in F_k are then understood as general emergent phenomena due to the transport of quasiparticle modes over large-scale distances set by the initial domain length N. For free fermions, where transport is ballistic, the onset of the two phases can be tuned by scaling the probing time τ linearly with N. The mapping presented here and the resulting thermodynamic phases are fundamentally different from those discussed for a single qubit in Refs. [55,56], where the long-range interaction emerges only for weak measurements. Accordingly, phase transitions in the measurement output of single qubits cannot be observed for purely projective measurements, in stark contrast with what is predicted here for many-body systems. Our analytical predictions highlight the rich impact of many-body quantum dynamics on FDRT and a deep connection between nonequilibrium measurement-induced quantum fluctuations and equilibrium thermodynamic phases.

Quantum first detected return and statistical mechanics. The FDRT probability of many-body systems described by a Hamiltonian $\mathcal{H}$, with associated unitary evolution $U(t) = e^{-i\mathcal{H}t}$, can be tackled by extending the formalism developed in Refs. [22,23,26,27] to the many-body realm, see Fig. 2(a). Right before the first measurement at time τ, the overlap of the wave function $|\Psi(\tau^-)\rangle = U(\tau)|\Psi(0)\rangle$ with the target state $|\Psi(0)\rangle$ is given by the Loschmidt amplitude

$$\mathcal{L}(\tau) = \langle\Psi(0)|U(\tau)|\Psi(0)\rangle, \tag{1}$$

and therefore the detection in $|\Psi(0)\rangle$ is successful with probability $F_1 = |\mathcal{L}(\tau)|^2$. In this case, one has $|\Psi(\tau^+)\rangle = |\Psi(0)\rangle$. If the detection is, instead, unsuccessful, the wave function is projected onto the space orthogonal to the target state $|\Psi(\tau^+)\rangle = (\mathbb{1} - \hat{P})|\Psi(\tau^-)\rangle/\sqrt{1 - F_1}$, where $\hat{P} = |\Psi(0)\rangle\langle\Psi(0)|$ such that $\langle\Psi(\tau^+)|\Psi(\tau^+)\rangle = 1$. Until the next measurement, i.e., for $\tau < t < 2\tau$ the state evolves unitarily, whence the procedure is repeated until the first detection in the target state occurs. The overlap between the target state and the unnormalized wave function after $k - 1$ unsuccessful detections evolved until immediately before the kth measurement defines the *first detection amplitude*,

$$\phi_k = \langle\Psi(0)|U(\tau)[(\mathbb{1} - \hat{P})U(\tau)]^{k-1}|\Psi(0)\rangle. \tag{2}$$

The FDRT probability F_k is given by $F_k = |\phi_k|^2$. The generating function $\hat{\phi}(z) = \sum_{k\geqslant 1}\phi_k z^k$ of ϕ_k is related to that $\hat{\mathcal{L}}(z) = \sum_{k\geqslant 1}\mathcal{L}_k z^k$ of $\mathcal{L}_k \equiv \mathcal{L}(k\tau)$ by [22,24,26]

$$\hat{\phi}(z) = \frac{\hat{\mathcal{L}}(z)}{1 + \hat{\mathcal{L}}(z)}. \tag{3}$$

The ϕ_k's are then determined as the integral

$$\phi_k = \oint \frac{\mathrm{d}z}{2\pi i}\frac{\hat{\phi}(z)}{z^{k+1}}, \tag{4}$$

along a contour enclosing the origin $z = 0$ and within the domain of analyticity of $\hat{\phi}(z)$.

By expanding the $(k-1)$th power of $(\mathbb{1} - \hat{P})U(\tau)$ in Eq. (2), one finds that ϕ_k can be written as

$$\phi_k = \sum_{r=1}^{k}(-1)^{r+1}\sum_{\ell_1,\ell_2,\ldots,\ell_r=1}^{\infty}\left(\prod_{j=1}^{r}\mathcal{L}_{\ell_j}\right)\delta_{\sum_{j=1}^{r}\ell_j,k}. \tag{5}$$

Equation (5) is crucial to map the problem into the partition function of a classical lattice spin model with noninteracting domains, as sketched in Fig. 2(b). A configuration of the spin model corresponds to a partition of the total volume k into r consecutive domains of lengths $\ell_1, \ldots, \ell_r$, with $\ell_1 + \cdots + \ell_r = k$ (see Fig. 2). Each domain has an associated length-dependent energy $E(\ell)$ resulting from the possibly long-range interactions among the spins within the domain. The "Boltzmann weight" w is associated, instead, to each domain wall. The canonical partition function of this model with fixed volume k can be written as

$$Z(k, w) = \sum_{r=1}^{k} w^{r+1}\sum_{\ell_1,\ell_2,\ldots,\ell_r=1}^{\infty}\left(\prod_{j=1}^{r}e^{-E(\ell_j)}\right)\delta_{\sum_{j=1}^{r}\ell_j,k}. \tag{6}$$

It is then apparent that Eq. (5) can be recovered from Eq. (6) by letting $w \to -1$ and by identifying the Loschmidt amplitude $\mathcal{L}_\ell = \mathcal{L}(\ell\tau)$ in time with the Boltzmann factor $e^{-E(\ell)}$ in space. Differently from the classical model, $E(\ell) = -\ln \mathcal{L}(\ell\tau)$ may now take complex values depending on the sign of $\mathcal{L}_\ell$, while $w = -1$ implies a purely imaginary energetic cost associated to a domain wall; these differences give rise to interferences when summed over, reflecting the quantum nature of ϕ_k. The analogy extends to the fixed-pressure grand canonical ensemble. Summing over the length k, one obtains the partition function

$$\mathcal{Z}(z, w) = \sum_{k=1}^{\infty} z^k Z(k, w) = \frac{w^2 \hat{\mathcal{L}}(z)}{1 - w\hat{\mathcal{L}}(z)}, \tag{7}$$

where z is the exponential of the pressure conjugate to the volume k, while $\hat{\mathcal{L}}(z) = \sum_{k\geqslant 1} e^{-E(k)} z^k$ is the grand canonical partition function of a single domain. Setting $w \to -1$ in Eq. (7), one recovers $\hat{\phi}(z)$ given in Eq. (3).

Emergence of thermodynamic phases. In the thermodynamic limit $k \to \infty$, the spin model introduced in Eq. (6) may exhibit, depending on the form of $E(\ell)$ and on the value of w, either a ferromagnetic or a paramagnetic phase [50–53]. This may happen even in one spatial dimension since $E(\ell)$ results from possibly long-range interactions among the spins within the domain. In the former case, the equilibrium ensemble is dominated by a globally ordered spin domain of length $\ell \sim O(k)$, while in the latter by disordered spins with $\ell \sim O(1)$. Identifying $\hat{\phi}(z)$ as $\mathcal{Z}(z, w \to -1)$ allows us to establish the possibility of observing two different behaviors of ϕ_k at large k, as shown in Fig. 2(c). If the spin model is in the ferromagnetic phase, the dominant configuration is a single, extended domain and thus $Z(k, -1) \sim e^{-E(k)}$; according to the mapping, this corresponds to the leading term of the first detection amplitude being $\phi_k \sim \mathcal{L}(k\tau)$. If the spin model is, instead, in the paramagnetic phase, and therefore it displays disordered domains, the partition function is dominated by many short domains $Z(k, -1) \sim e^{-kE(1)}$. In terms of the quantum evolution, this corresponds to $\phi_k \sim [\mathcal{L}(\tau)]^k$.

The two cases mentioned above are understood through the analytic properties of $\hat{\phi}(z) = \mathcal{Z}(z, -1)$ as a function of z which determines ϕ_k according to Eq. (4). The radius of convergence of $\hat{\phi}$ is controlled by its closest singularity z^* to the origin. By inspection of Eqs. (3) and (7), the singular point z^* may arise from either (i) a root in the denominator, i.e., $1 + \hat{\mathcal{L}}(z^*) = 0$, leading to a simple pole, or (ii) a nonanalyticity in $\hat{\mathcal{L}}(z^*)$ leading to a branch point. If the singularity at z^* is a simple pole, $\hat{\phi}(z) \sim (z - z^*)^{-1}$, the integration in Eq. (4) renders $\phi_k \sim (z^*)^{-k}$ and therefore an exponential dependence of ϕ_k on k. This exponential decay corresponds to the configuration with k domains, i.e., to the paramagnetic phase. If the singularity z^* is a branch point, instead, $\hat{\phi}(z) \sim |z - z^*|^{c-1}$ and, via Tauberian theorems, one obtains from (4) an algebraic decay of $\phi_k \sim k^{-c}$ for large k [57]. Algebraic growth of a canonical partition function as a function of the volume is a consequence of a single domain in a long-range interacting spin model and thus we associate this behavior with the ferromagnetic phase.

We illustrate this mapping by investigating the FDRT of N free fermions with Hamiltonian $\mathcal{H} = \sum_{j=-L}^{L} (c_j^\dagger c_{j+1} + c_{j+1}^\dagger c_j)$, where c_j ($c_j^\dagger$) is the fermionic annihilation (creation) operator at lattice site j. The system size L is henceforth taken to infinity $L \to \infty$. We consider an initial state $|\Psi(0)\rangle$ consisting of N adjacent fermions $|\Psi(0)\rangle = \otimes_{j=1}^{N} c_j^\dagger |0\rangle$, where $|0\rangle$ is the vacuum of the system [see the sketch in Fig. 1 and in Fig. 2(a)]. The case $N = \infty$ corresponds to a domain wall at site $j = 0$ separating the empty half-infinite chain from the complementary filled one [58,59]. The free-fermion model is motivated by recent implementation of quantum walks under stroboscopic measurements on quantum computers [40–42], where a qubit hopping Hamiltonian analogous to $\mathcal{H}$ above, with $N = 1$, is implemented.

Ferromagnetic phase for finite N. For finite N, $\mathcal{L}_k$ is the determinant of the matrix $\mathbb{J}_N(k\tau) = [i^{n-m} J_{m-n}(2k\tau)]_{m,n=1\ldots N}$, where $J_n(x)$ is the nth Bessel function of the first kind [60]. For large times $k\tau$, the determinant $\mathcal{L}_k$ decays algebraically [60,61]. According to the mapping discussed above, the energy cost $E(\ell) = -\ln \mathcal{L}(\ell\tau)$ of a domain is logarithmic in ℓ

$$E(\ell) = c_N \ln \ell + \Delta_N + (N \bmod 2) \ln \cos(2\ell\tau - N\pi/4), \tag{8}$$

where we introduced $c_N = (N^2 + N \bmod 2)/4$. The definition of Δ_N is reported in the Supplemental Material [61,62]. Introducing the fugacity $y = e^{-\Delta_N}$, the grand canonical partition function of the spin model in Eq. (7) reads

$$\mathcal{Z}_N(z, w) = \frac{w^2 y \Lambda_N(z)}{1 - wy\Lambda_N(z)}, \tag{9}$$

where $\Lambda_N(z)$ is determined in terms of the polylogarithm function [61]. For $w = 1$ and N even, Eq. (9) equals the partition function of the truncated inverse distance squared Ising model (TIDSI) [50] which is parametrized by y and c_N. In TIDSI model, spins within the same domain experience a long-range interaction $\sim r^{-2}$ as a function of their mutual distance r. In the quantum problem, these long-range interactions allow the emergence of a ferromagnetic phase for purely projective measurements. Namely, the TIDSI model undergoes a mixed-order phase transition from a paramagnetic to a ferromagnetic phase [50–53]. In the quantum picture, however, we consider the partition function $\mathcal{Z}(z, w)$ at $w = -1$. For the spin model, this corresponds to studying the TIDSI model at the (classically forbidden) negative fugacity $-y$.

The leading singularity of $\mathcal{Z}_N$ in Eq. (9) is due to branch points [61,63,64]. The integral in Eq. (4) can then be worked out for all N, from which one obtains the leading large-k behavior of ϕ_k. For $N = 1$, our analysis renders the result $F_k \sim k^{-3}$ of Ref. [27]. For $N > 1$, instead, it gives, up to some oscillating prefactor, $\phi_k \sim \mathcal{L}_k$ and thus the algebraic decay

$$\phi_k \sim k^{-c_N} \quad \text{and} \quad F_k \sim k^{-2c_N}, \tag{10}$$

with logarithmic corrections $\phi_k \sim (\ln k)^n / k^{c_N}$ of all integer orders $n \geqslant 1$ for $N = 2$ [61]. This algebraic behavior is consistent with a ferromagnetic, globally ordered phase in the spin model. One can intuitively understand this as a consequence of the logarithmically slow growth of the domain energy $E(\ell)$ in length ℓ, which renders a global ordering thermodynamically favorable in the large k limit and

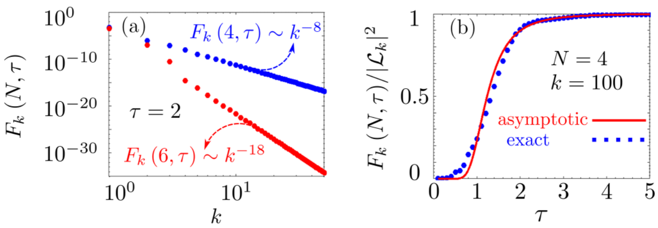

FIG. 3. Ferromagnetic phase: algebraic decay. (a) Log-log plot of the first detected return time probability F_k as a function of k for fixed stroboscopic time $\tau = 2$, with $N = 4$ and 6. $F_k \sim |\mathcal{L}_k|^2 \sim k^{-2c_N}$ (with $c_4 = 4$ and $c_6 = 9$) decays algebraically upon increasing k according to the mapping to the ferromagnetic phase of the spin model. (b) Ratio $F_k/|\mathcal{L}_k|^2$ (blue dots) as a function of τ, for fixed $k = 100$ and $N = 4$ compared with the branch-cut asymptotic (red solid line).

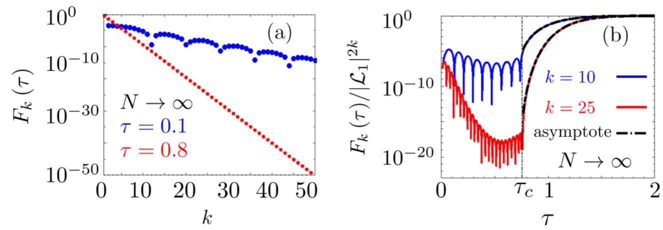

FIG. 4. Paramagnetic phase: exponential decay. (a) Log-linear plot of the first detected return time probability $F_k(\tau) \equiv F_k(N = \infty, \tau)$ of the semi-infinite occupied line as a function of k for stroboscopic times $\tau = 0.1$ (top-blue dotted) and 0.8 (bottom-red dashed). F_k decays exponentially upon increasing k, according to the mapping to the paramagnetic phase of the spin model. This exponential decay holds for all values of τ. For $\tau < \tau_c = 0.77\ldots$, F_k features additional oscillations (blue symbols). (b) Log-linear plot of the ratio $F_k(\tau)/|\mathcal{L}_1|^{2k}$ as a function of τ for fixed values of $k = 10$ and 25. This ratio, for $\tau > \tau_c$, is well approximated by the systematic expansion (dot-dashed lines) mentioned in the main text. For $\tau < \tau_c$, instead, the asymptotics break down and $F_k(\tau)$ displays $k - 2$ positive roots as a function of τ.

therefore $\phi_k \sim \mathcal{L}_k$. In Fig. 3(a), we show the exact FDRT probabilities F_k for $N = 4$ and 6 [61], with fixed $\tau = 2$, as obtained from the exactly known Loschmidt echo, which are compared with the expected leading algebraic behavior (10), showing excellent agreement for large k. Figure 3(b) shows that the ratio $F_k/|\mathcal{L}_k|^2$ is well captured by the branch cut asymptotics for intermediate values of $\tau \gtrsim 1.8$ and large values of k.

Paramagnetic phase for $N = \infty$. For an half-infinite domain, i.e., for $N = \infty$, the Loschmidt amplitude is exactly given by $\mathcal{L}(\tau) = e^{-\tau^2}$ [58,59]. In the spin model this corresponds to a quadratic energetic cost of a domain: $E(\ell) = \tau^2\ell^2$. In order to evaluate $\mathcal{Z}_N(z, w)$ in Eq. (7), we introduce a partial theta function [65] $\Theta_+(z, q) = \sum_{k=1}^{\infty} z^k q^{k^2}$ in terms of which $\hat{\mathcal{L}}(z) = \Theta_+(z, e^{-\tau^2})$. The grand canonical partition function is

$$\mathcal{Z}_\infty(z, w) = \frac{w^2\Theta_+(z, e^{-\tau^2})}{1 - w\Theta_+(z, e^{-\tau^2})}. \tag{11}$$

For all $q \in (0, 1)$, $\Theta_+(z, q)$ is an analytic function of z [66], thus excluding branch cuts. In turn, for $w = -1$, $\mathcal{Z}_\infty$ has a countable set of poles at the complex roots z_n of $1 + \Theta_+(z_n, q) = 0$ [67]. For $q^{-2} \geqslant q_\infty = 3.23\ldots$, these roots are simple, real, and negative [68,69], and they are approximately given, for large n, by $z_n = -q^{1-2n}$ [70]. This implies that for $\tau \geqslant \tau_c = \sqrt{(\ln q_\infty)/2} = 0.77\ldots$ the contour integral in Eq. (4) is dominated, for large k, by the simple pole $z^* = z_1$ closest to the origin. One then finds $\phi_k \sim (z^*)^{-k}$ for $\tau > \tau_c$ with a k-independent prefactor. This exponential decay is shown in Fig. 4(a) for $\tau = 0.8 > \tau_c$. This behavior corresponds to the paramagnetic phase in the spin model and can therefore be explained with the stronger quadratic growth of $E(\ell)$ upon increasing ℓ, compared to the logarithmic growth (8) for finite N. For $\tau < \tau_c$, the poles of $\mathcal{Z}_\infty$ are complex conjugate and therefore F_k displays oscillations as a function of k. This is illustrated in Fig. 4(a) for $\tau = 0.1 < \tau_c$. The critical value τ_c is not related to the energy bandwidth of the model and it is therefore a fundamentally novel feature compared to the "resonant probing times" [27,61] occurring at finite N. The asymptotics of $F_k/|\mathcal{L}_1|^{2k}$ for $\tau > \tau_c$ can be obtained by applying Faà di Bruno's theorem [71,72] to $\mathcal{Z}_\infty$, which amounts at performing an expansion in the maximal domain length ℓ_M considered [61,71,72]. The estimates with $\ell_M = 3$ are compared in Fig. 4(b) with the exact predictions for $F_k/|\mathcal{L}_1|^{2k}$, showing excellent agreement. As $\tau \to 0$ the quantum Zeno regime is met. Surprisingly, we observe [61] that, correspondingly, $F_k(N, \tau)$ coincides with $F_k(N \to \infty, \tau)$ for every value of the particle number N.

Phase crossover and ferromagnetic transition. We investigate here the onset of the ferromagnetic phase in F_k upon increasing k beyond a crossover volume k_{cr}. For sufficiently small $k < k_{\text{cr}}$, F_k is in perfect agreement with the paramagnetic behavior observed for $N = \infty$ fermions and predicted by $\mathcal{Z}_\infty(k, -1)$ in Eq. (11). Upon increasing k beyond k_{cr}, instead, F_k sharply crosses over into the ferromagnetic behavior predicted by Eq. (9), where $F_k \sim |\mathcal{L}_k|^2$. This crossover is illustrated in Fig. 5(a) for $N = 6$ and $\tau = 1$. Note that, upon increasing τ, the initial exponential decay might not be visible, as it happens in Fig. 3(a) with $\tau = 2$, where only the eventual algebraic behavior is seen. In a complementary way, Fig. 5(b) shows that for a fixed value of $k = 10$, larger values of $\tau > \tau_{\text{cr}}$ are needed in order for F_k to be described by the ferromagnetic partition function in Eq. (9).

For large N, this crossover from paramagnetic to ferromagnetic behavior can be rationalized by studying the scaling limit of the Loschmidt amplitude $\mathcal{L}(\tau)$. Keeping $x = \tau/N$ finite, $\mathcal{L}(\tau)$ satisfies $\lim_{N\to\infty} N^{-2} \ln \mathcal{L}(Nx) = -f(x)$ where, up to oscillating factors for N odd, $f(x) \approx (\ln x)/4 + 3/8$ for $x \gg 1$ and $f(x) \approx x^2$ for $x \ll 1$ [60]. This fact implies that, upon rescaling the stroboscopic time τ with the number N of fermions, the energy $E(k) = N^2 f(k\tau/N)$ associated to a domain in the spin model may either grow logarithmically or quadratically as a function of k. We conclude that the typical crossover chain volume $(k\tau)_{\text{cr}}$, above which F_k decays algebraically, satisfies $(k\tau)_{\text{cr}} \sim N$ [61]. We emphasize that crossover from paramagnetic to ferromagnetic decay is a general phenomenon caused by the transport of quasiparticles over the macroscopic distance N set by the initial domain-wall state. The only specific aspect to free fermions is provided by the linear scaling between space and time due to the associated ballistic transport [58,73–82].

Summary and outlook. We derived exact analytical predictions for the first detected return time (FDRT) of many-body quantum systems by mapping the FDRT onto the partition function of a classical system of magnetic domains in one spatial dimension. This mapping provides a physical explanation of the rich behavior of the probability of the FDRT which may display an algebraic (ferromagnetic) or an exponential (paramagnetic) decay at long times. Our results are valid for an arbitrarily large number N of particles, including the limit $N \to \infty$. The onset of the algebraic decay can be remarkably controlled by scaling the stroboscopic time τ with the number N of particles, making such a decay accessible already for small values of k, when F_k is still significant. This fact is crucial for actual implementations of the protocol discussed here on quantum computer platforms as in Refs. [40–42]. Therein, indeed, F_k at small values of k can be measured with great accuracy for a small number $N = 2, 3, 4$ of particles and rings of finite length L. The present analysis therefore paves the way for investigations of collective effects in multiparticle quantum walks via quantum computers. Upon increasing k, the probability F_k becomes rapidly small since the initial inhomogeneous domain-wall state evolves towards an homogeneous density profile [83]. In order to devise efficient detection protocols, it is then very interesting to introduce resetting [36,38,39,84–90] after a sequence of unsuccessful detections. Similarly, a very promising avenue is provided by models featuring Wannier-Stark localization [91–93] or quantum many-body scars [94–98]. In both the cases, the Loschmidt echo shows perfect revivals in time. In the former, this happens for generic initial and target states due to Bloch oscillations induced the confining field. In the latter, revivals are present only when the initial and target state of detection belong to the scarred subspace, since the corresponding energy levels are equispaced. These revivals can then be exploited in order to obtain an enhanced FDRT sensing for large times k. In addition, it would be interesting to extend the many-body first detection protocol to weak measurements, which have been so far studied [55,56] only for single-qubit systems.

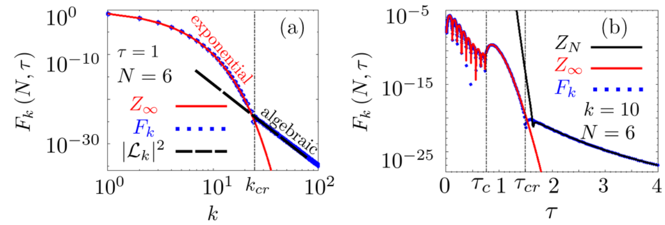

FIG. 5. Phase crossover. (a) Log-log plot of the first detection probability $F_k(N, \tau)$ as a function of k for a fixed $\tau = 1$ and $N = 6$. Upon increasing k, F_k shows a crossover from an exponential-paramagnetic to an algebraic-ferromagnetic decay. In this panel, the crossover occurs at $k = k_{\mathrm{cr}} \approx 25$ for $N = 6$, where $k_{\mathrm{cr}} \sim N/\tau$. (b) Log-linear plot of $F_k(N, \tau)$ as a function of τ for fixed $k = 10$ and for $N = 6$ fermions. For $\tau < \tau_{\mathrm{cr}}$, with $\tau_{\mathrm{cr}} \approx 1.5$ and $\tau_{\mathrm{cr}} \sim N/k$, F_k (blue dots) coincides with the paramagnetic partition function $|Z_\infty(k, -1)|^2$ (red line), while for $\tau > \tau_{\mathrm{cr}}$, $F_k(\tau)$ coincides, up to some proportionality factor, with the ferromagnetic partition function $|Z_N(k, -1)|^2$ (black line). The crossover stroboscopic time scales as $\tau_{\mathrm{cr}} \sim N/k$ upon increasing N.

Acknowledgments. The authors would like to thank Eli Barkai for fruitful discussions and helpful comments. B.W. would like to thank Giorgio Li, Adam Nahum, and Kay Wiese for insightful discussions. B.W. and A.G. acknowledge support from MIUR PRIN project "Coarse-grained description for non-equilibrium systems and transport phenomena (CO-NEST)" No. 201798CZL. B.W. acknowledges funding from the Imperial College Borland Research Fellowship. G.P. acknowledges support from the Alexander von Humboldt foundation through a Humboldt research fellowship for postdoctoral researchers. A.G. acknowledges support of PNRR MUR Project No. PE0000023-NQSTI.

Data availability. The code and the data that support the findings of this Letter are available on Zenodo [99].

[1] I. Bloch, J. Dalibard, and S. Nascimbène, Nat. Phys. **8**, 267 (2012).
[2] I. M. Georgescu, S. Ashhab, and F. Nori, Rev. Mod. Phys. **86**, 153 (2014).
[3] A. Browaeys and T. Lahaye, Nat. Phys. **16**, 132 (2020).
[4] C. Monroe, W. C. Campbell, L.-M. Duan *et al.*, Rev. Mod. Phys. **93**, 025001 (2021).
[5] E. Altman, K. R. Brown, G. Carleo *et al.*, PRX Quantum **2**, 017003 (2021).
[6] H. J. Briegel, D. E. Browne, W. Dür, R. Raussendorf, and M. Van den Nest, Nat. Phys. **5**, 19 (2009).
[7] B. P. Lanyon, P. Jurcevic, M. Zwerger, C. Hempel, E. A. Martinez, W. Dür, H. J. Briegel, R. Blatt, and C. F. Roos, Phys. Rev. Lett. **111**, 210501 (2013).
[8] L. Aolita, F. de Melo, and L. Davidovich, Rep. Prog. Phys. **78**, 042001 (2015).
[9] F. Arute, K. Arya, R. Babbush *et al.*, Nature (London) **574**, 505 (2019).
[10] R. J. Lewis-Swan, A. Safavi-Naini, A. M. Kaufman, and A. M. Rey, Nat. Rev. Phys. **1**, 627 (2019).
[11] A. Chan, R. M. Nandkishore, M. Pretko, and G. Smith, Phys. Rev. B **99**, 224307 (2019).
[12] B. Skinner, J. Ruhman, and A. Nahum, Phys. Rev. X **9**, 031009 (2019).
[13] A. C. Potter and R. Vasseur, *Entanglement in Spin Chains: From Theory to Quantum Technology Applications*, edited by A. Bayat, S. Bose, and H. Johannesson (Springer, Cham, 2022), pp. 211–249.
[14] M. P. A. Fisher, V. Khemani, A. Nahum, and S. Vijay, Annu. Rev. Condens. Matter Phys. **14**, 335 (2023).
[15] M. A. Nielsen and I. L. Chuang, *Quantum Computation and Quantum Information*, 10th ed. (Cambridge University Press, Cambridge, UK, 2010).
[16] A. M. Childs, D. Gosset, and Z. Webb, Science **339**, 791 (2013).
[17] L. W. Cheuk, M. A. Nichols, M. Okan, T. Gersdorf, V. V. Ramasesh, W. S. Bakr, T. Lompe, and M. W. Zwierlein, Phys. Rev. Lett. **114**, 193001 (2015).
[18] S. Nakayama, A. Soeda, and M. Murao, Phys. Rev. Lett. **114**, 190501 (2015).

[19] F. Schäfer, T. Fukuhara, S. Sugawa, Y. Takasu, and Y. Takahashi, Nat. Rev. Phys. **2**, 411 (2020).
[20] C. Gross and W. S. Bakr, Nat. Phys. **17**, 1316 (2021).
[21] H. Krovi and T. A. Brun, Phys. Rev. A **74**, 042334 (2006).
[22] F. A. Grünbaum, L. Velázquez, A. H. Werner, and R. F. Werner, Commun. Math. Phys. **320**, 543 (2013).
[23] S. Dhar, S. Dasgupta, and A. Dhar, J. Phys. A: Math. Theor. **48**, 115304 (2015).
[24] S. Dhar, S. Dasgupta, A. Dhar, and D. Sen, Phys. Rev. A **91**, 062115 (2015).
[25] P. Sinkovicz, Z. Kurucz, T. Kiss, and J. K. Asbóth, Phys. Rev. A **91**, 042108 (2015).
[26] H. Friedman, D. A. Kessler, and E. Barkai, J. Phys. A: Math. Theor. **50**, 04LT01 (2017).
[27] H. Friedman, D. A. Kessler, and E. Barkai, Phys. Rev. E **95**, 032141 (2017).
[28] F. Thiel, D. A. Kessler, and E. Barkai, Phys. Rev. A **97**, 062105 (2018).
[29] F. Thiel, E. Barkai, and D. A. Kessler, Phys. Rev. Lett. **120**, 040502 (2018).
[30] F. Thiel, I. Mualem, D. A. Kessler, and E. Barkai, arXiv:1909.02114.
[31] Q. Liu, R. Yin, K. Ziegler, and E. Barkai, Phys. Rev. Res. **2**, 033113 (2020).
[32] F. Thiel, I. Mualem, D. Meidan, E. Barkai, and D. A. Kessler, Phys. Rev. Res. **2**, 043107 (2020).
[33] F. Thiel and D. A. Kessler, Phys. Rev. A **102**, 012218 (2020).
[34] V. Dubey, C. Bernardin, and A. Dhar, Phys. Rev. A **103**, 032221 (2021).
[35] D. Das and S. Gupta, J. Stat. Mech. (2022) 033212.
[36] R. Yin and E. Barkai, Phys. Rev. Lett. **130**, 050802 (2023).
[37] R. Yin and E. Barkai, Q. Wang, Phys. Rev. E **109**, 064150 (2024).
[38] M. Kulkarni and S. N. Majumdar, J. Phys. A: Math. Theor. **56**, 385003 (2023).
[39] P. Chatterjee, S. Aravinda, and R. Modak, Phys. Rev. E **110**, 034132 (2024).
[40] R. Yin, Q. Wang, S. Tornow, and E. Barkai, Proc. Natl. Acad. Sci. USA **122**, e2402912121 (2025).
[41] Q. Wang, S. Ren, R. Yin, K. Ziegler, E. Barkai, and S. Tornow, Entropy **26**, 869 (2024).
[42] S. Tornow and K. Ziegler, Phys. Rev. Res. **5**, 033089 (2023).
[43] Q. Liu, D. A. Kessler, and E. Barkai, arXiv:2401.09810.
[44] C. Dittel, N. Neubrand, F. Thiel, and A. Buchleitner, Phys. Rev. A **107**, 052206 (2023).
[45] A. Purkayastha and A. Imparato, Phys. Rev. A **109**, L020202 (2024).
[46] D. Poland and H. A. Scheraga, J. Chem. Phys. **45**, 1456 (1966).
[47] D. Poland and H. A. Scheraga, J Chem Phys **45**, 1464 (1966).
[48] M. E. Fisher, J. Stat. Phys. **34**, 667 (1984).
[49] C. Richard and A. J. Guttmann, J. Stat. Phys. **115**, 925 (2004).
[50] A. Bar and D. Mukamel, Phys. Rev. Lett. **112**, 015701 (2014).
[51] A. Bar and D. Mukamel, J. Stat. Mech. (2014) P11001.
[52] M. Barma, S. N. Majumdar, and D. Mukamel, J. Phys. A: Math. Theor. **52**, 254001 (2019).
[53] D. Mukamel, *50 Years of the Renormalization Group* (World Scientific, Singapore, 2025), Chap. 10, pp. 89–101.
[54] R. J. Harris and H. Touchette, J. Phys. A: Math. Theor. **50**, 10LT01 (2017).
[55] W.-L. Ma, P. Wang, W.-H. Leong, and R.-B. Liu, Phys. Rev. A **98**, 012117 (2018).
[56] X. Tang and F. Li, Phys. Rev. A **101**, 062102 (2020).
[57] P. Flajolet and R. Sedgewick, *Analytic Combinatorics*, 1st ed. (Cambridge University Press, Cambridge, U.K., 2009).
[58] J. Viti, J.-M. Stéphan, J. Dubail, and M. Haque, Europhys. Lett. **115**, 40011 (2016).
[59] L. Wei, R.-A. Pitaval, J. Corander, and O. Tirkkonen, IEEE Trans. Inf. Theory **63**, 2814 (2017).
[60] P. L. Krapivsky, J. M. Luck, and K. Mallick, J. Stat. Mech. (2018) 023104.
[61] See Supplemental Material at http://link.aps.org/supplemental/10.1103/PhysRevA.111.L040202 for the details of the calculations.
[62] E. W. Barnes, Philos. Trans. R. Soc. A **196**, 265 (1901).
[63] H. Bateman and A. Erdélyi, *Higher Transcendental Functions*, California Institute of Technology. Bateman Manuscript Project (McGraw-Hill, New York, NY, 1953).
[64] DLMF, NIST Digital Library of Mathematical Functions, edited by F. W. J. Olver, A. B. Olde Daalhuis, D. W. Lozier, B. I. Schneider, R. F. Boisvert, C. W. Clark, B. R. Miller, B. V. Saunders, H. S. Cohl, and M. A. McClain, https://dlmf.nist.gov/.
[65] G. E. Andrews, Adv. Math. **41**, 137 (1981).
[66] V. Kostov, Mat. Stud. **58**, 142 (2023).
[67] G. H. Hardy, Proc. London Math. Soc. **s2-2**, 332 (1905).
[68] O. M. Katkova, T. Lobova, and A. M. Vishnyakova, Comput. Methods Funct. Theory **3**, 425 (2004).
[69] V. P. Kostov and B. Shapiro, Duke Math. J. **162**, 825 (2013).
[70] J. I. Hutchinson, Trans. Am. Math. Soc. **25**, 325 (1923).
[71] H. Gould, *Combinatorial Identities: A Standardized Set of Tables Listing 500 Binomial Coefficient Summations* (Morgantown Printing, Morgantown, WV, 1972).
[72] L. Comtet, *Advanced Combinatorics* (Springer, Dordrecht, 1974).
[73] T. Antal, Z. Rácz, A. Rákos, and G. M. Schütz, Phys. Rev. E **59**, 4912 (1999).
[74] T. Platini and D. Karevski, Eur. Phys. J. B **48**, 225 (2005).
[75] M. Collura and G. Martelloni, J. Stat. Mech. (2014) P08006.
[76] N. Allegra, J. Dubail, J.-M. Stéphan, and J. Viti, J. Stat. Mech. (2016) 053108.
[77] B. Bertini and M. Fagotti, Phys. Rev. Lett. **117**, 130402 (2016).
[78] V. Eisler, F. Maislinger, and H. G. Evertz, SciPost Phys. **1**, 014 (2016).
[79] M. Kormos, SciPost Phys. **3**, 020 (2017).
[80] G. Perfetto and A. Gambassi, Phys. Rev. E **96**, 012138 (2017).
[81] M. Ljubotina, S. Sotiriadis, and T. Prosen, SciPost Phys. **6**, 004 (2019).
[82] G. Perfetto and A. Gambassi, Phys. Rev. E **102**, 042128 (2020).
[83] H. Tasaki, arXiv:2404.04533.
[84] B. Mukherjee, K. Sengupta, and S. N. Majumdar, Phys. Rev. B **98**, 104309 (2018).
[85] A. Riera-Campeny, J. Ollé, and A. Masó-Puigdellosas, arXiv:2011.04403.
[86] G. Perfetto, F. Carollo, M. Magoni, and I. Lesanovsky, Phys. Rev. B **104**, L180302 (2021).
[87] G. Perfetto, F. Carollo, and I. Lesanovsky, SciPost Phys. **13**, 079 (2022).
[88] X. Turkeshi, M. Dalmonte, R. Fazio, and M. Schirò, Phys. Rev. B **105**, L241114 (2022).

[89] M. Magoni, F. Carollo, G. Perfetto, and I. Lesanovsky, Phys. Rev. A **106**, 052210 (2022).
[90] S. Belan and V. Parfenyev, New J. Phys. **22**, 073065 (2020).
[91] G. H. Wannier, Phys. Rev. **117**, 432 (1960).
[92] H. Fukuyama, R. A. Bari, and H. C. Fogedby, Phys. Rev. B **8**, 5579 (1973).
[93] T. Hartmann, F. Keck, H. Korsch, and S. Mossmann, New J. Phys. **6**, 2 (2004).
[94] D. K. Mark, C.-J. Lin, and O. I. Motrunich, Phys. Rev. B **101**, 195131 (2020).
[95] S. Moudgalya, B. A. Bernevig, and N. Regnault, Rep. Prog. Phys. **85**, 086501 (2022).
[96] A. Chandran, T. Iadecola, V. Khemani, and R. Moessner, Annu. Rev. Condens. Matter Phys. **14**, 443 (2023).
[97] O. Vafek, N. Regnault, and B. A. Bernevig, SciPost Phys. **3**, 043 (2017).
[98] M. Schecter and T. Iadecola, Phys. Rev. Lett. **123**, 147201 (2019).
[99] B. Walter, G. Perfetto, and A. Gambassi, Data of "Thermodynamic phases in first detected return times of quantum many-body systems", Zenodo (2025), doi:10.5281/zenodo.15040459.